Radiochim. Acta **100**, 189–195 (2012) / **DOI** 10.1524/ract.2012.1900

Site-selective time resolved laser fluorescence spectroscopy of Eu and Cm doped $LaPO_4$

By K. S. Holliday[1,*], C. Babelot[2], C. Walther[1], S. Neumeier[2], D. Bosbach[2] and Th. Stumpf[1,3]

[1] Karlsruhe Institut für Technologie, Institut für Nukleare Entsorgung, P.O. Box 3640, 76021 Karlsruhe, Germany
[2] Institut für Energie- und Klimaforschung – Nukleare Entsorgung und Reaktorsicherheit (IEK-6), Forschungszentrum Jülich GmbH, 52425 Jülich, Germany
[3] Karlsruhe Institut für Technologie, Institut für Anorganische Chemie, Engesserstr. 15, 76131 Karlsruhe, Germany

(Received March 4, 2011; accepted in revised form July 22, 2011)

Lanthanum phosphate / TRLFS / Europium / Site-selective / Curium

Summary. Samples of $LaPO_4$ doped with Eu^{3+} or Cm^{3+} were synthesized by a hydrothermal process which resulted in a solid solution at temperatures less than conventional processing. Time resolved laser fluorescence spectroscopy was used to probe the incorporated Eu^{3+} or Cm^{3+} in order to gain structural information on its local environment. This revealed that Eu^{3+} and Cm^{3+} incorporate on the La site as expected. The emission spectrum of Eu^{3+} resolves the fully degenerate 5-fold splitting of the peaks in the F_2 transition due to the low symmetry of the site, confirming previous calculations. A minor site in the Eu^{3+} doped sample is identified as coordinated with hydroxide contamination. Direct excitation of Cm^{3+} doped samples show the presence of "satellite" species. Although these spectral features have been observed in Cm^{3+} doped $LuPO_4$ and YPO_4, this is the first time that these satellites are resolved into their individual species. These are hypothesized to be due to a disturbance in the ideal structure which creates a break in the equivalence of the four lanthanum sites within a unit cell. The 4-fold ground state splitting of all species is identical, although slightly shifted, indicating similar environments. The fluorescence lifetimes were long (1.2 ms for Cm and 3.6 ms for Eu) indicating an absence of water in the immediate coordination sphere due to the incorporation of the doping ion.

1. Introduction

Much progress has been made on improving waste forms for the long term storage of nuclear waste. Advances in partitioning have provided the opportunity for waste forms that address a selection of elements instead of the whole of nuclear waste [1]. This makes it possible to develop ceramic waste forms of superior stability as compared to borosilicate glass, which is accepted as the first generation waste form [2–4]. One particular waste stream that will require long term storage in a nuclear waste repository is the transuranics including americium, curium and plutonium. These elements contribute significantly to the radiotoxicity of nuclear waste at long time periods (> 1000 years) [5].

One possible ceramic that shows promise as a waste form for actinides is the monazite $LaPO_4$. The monazite crystal structure is able to incorporate trivalent actinides such as Pu(III), Am(III), and Cm(III) to a high loading of up to 25 wt % [6, 7]. Also, monazite can form a solid solution with brabantite which allows it to incorporate tetravalent actinides such as U(IV) and Np(IV) [8, 9]. Monazites have proven to be extremely stable, with some deposits in Brazil dated as over two billion years old [4]. Natural monazite [10, 11] and $(La,An)PO_4$ [12] have been shown to be radiation tolerant to high alpha doses. This has been attributed to an alpha-annealing process that enables monazite to recover crystallinity under irradiation [13–16]. It has also been demonstrated that it is possible to synthesize single phase Pu and Am containing monazite in a method that can be adapted to a hot cell environment through the use of $NH_4H_2PO_4$ [7].

Monazite material has shown promise as a luminescent material for various applications when doped with rare earth elements such as Eu, Ce, Sm, Dy and Tb. Because of this, there have been many studies which report on the fluorescence properties of doped monazite materials [*e.g.* 17–21]. Few studies, however, report the fluorescence of these materials to a level that is useful for determining detailed structural information. A notable exception is Meyssamy *et al.* [22], which reports the time resolved laser fluorescence spectroscopy (TRLFS) of Eu, Ce, and Tb doped $LaPO_4$ along with the calculated emission lines for $Eu:LaPO_4$. Although these emission lines were fit to the emission spectra they are not clearly resolved in the experimental data [22].

An even larger void in reported data exists for minor actinides. Cavellec *et al.* [23] report on the Cm spectroscopy in several phosphate systems other than monazite. A detailed study of Cm^{3+} doped $LuPO_4$ and YPO_4 (xenotime structure) was performed by groups at ORNL, LBNL and ANL in the United States [24, 25]. Those studies found multiple "satellite" species of Cm^{3+} that were explained as resulting from different Cm^{3+} environments due to structural imperfections [24] or from electrons populating multiple levels of degenerate ground states due to sample self heating [25]. To date there has not been any such TRLFS study performed on the monazite $LaPO_4$ structure doped with Cm^{3+}.

The current study uses TRLFS of Eu^{3+} and Cm^{3+} as structural probes in $LaPO_4$. The Eu spectroscopy has been

---

[*] Author for correspondence (E-mail: holliday.kiel@gmail.com).

performed at a higher resolution than previously reported, confirming prior calculations [22]. Two minor sites were identified and the emission spectra are presented. TRLFS of Cm^{3+} doped $LaPO_4$ is examined for the first time in the current study. The results from TRLFS measurements are used in comparison to previously reported studies on $LuPO_4$:Cm in the xenotime structure [24, 25]. The structural information gained by the TRLFS of trivalent actinides and lanthanides in $LaPO_4$ will be used to better assess the long term performance of the proposed waste form and improve the understanding of fundamental interactions governing radionuclide migration.

2. Experimental

2.1 Sample preparation

The synthesis of $LaPO_4$ was based on the method developed by Meyssamy *et al.* [22]. High purity (99.99%) La_2O_3 and Eu_2O_3 were used to prevent emission from rare earth impurity ions. All other chemicals were reagent grade purchased from Alpha Aesar with the exception of Cm-248 ($t_{1/2} = 3.4 \times 10^5$ yr). The isotopic composition of the long-lived curium solution (20.0 μM) is 97.3% Cm-248, 2.6% Cm-246, 0.04% Cm-245, 0.02% Cm-247 and 0.009% Cm-244 in 1.0 M $HClO_4$.

A 0.6 M La solution doped with Eu (500–5000 ppm) was made by mixing the appropriate amount of oxide material and dissolving in a minimal amount of 10 M HNO_3 and diluting with water (18 MΩ cm). In the case of Cm, doping was achieved by adding the appropriate amount of Cm stock solution (2×10^{-5} M) to the La solution, prepared as above in the absence of Eu. A 4 mL aliquot of the prepared La solution was added to 8 mL of 1 M NaOH. To the well-stirred suspension, 8 mL of $(NH_4)_2HPO_4$ solution (0.27 M) was added. The pH was then adjusted to 12.5 with 4 M NaOH and the solution transferred to a Teflon-lined steel autoclave. The autoclave was then heated to 200 °C for 2 h in a box furnace. Once cool, the suspension was centrifuged and supernatant discarded. The solid was suspended in 25 mL of 0.1 M HNO_3 for 3 days in order to dissolve $La(OH)_3$ created by excess La under hydrothermal treatment. The resulting pure $LaPO_4$ solid was then recovered by centrifugation and dried at 90 °C overnight. Samples were analyzed before (as prepared) and after (sintered) heating to 1000 °C for 48 h in a box furnace under atmospheric conditions.

The solid product was confirmed to be $LaPO_4$ with the monazite crystal structure before and after sintering by X-ray diffraction (Bruker D8 Advance). The supernatant from the synthesis and acid wash was analyzed by ICP-MS to confirm that Eu or Cm did not remain in solution, but was in fact incorporated as a solid solution.

2.2 TRLFS (time resolved laser fluorescence spectroscopy)

TRLFS was performed using a pulsed (20 Hz) XeCl-eximer laser (Lambda Physics, EMG, 308 nm) pumped dye laser (Lambda Scanmate). The following dyes were used: QUI for UV excitation, Rhodamine 6G for direct excitation of Eu, and Rhodamine B for direct excitation of Cm. Indirect excitation of Eu and Cm was performed at 394 and 396.6 nm respectively. The range used for the direct excitation of Eu was 575–582 nm and the direct excitation of Cm was done at 600–604 nm. The laser wavelength was monitored using a Toptica WS7 wavemeter ($> 10^{-5}$ nm accuracy). Normal fluorescence measurements were detected by an optical multichannel analyzer that consists of a polychrometer with 300/600/1200 lines/mm gratings (Jobin Yvon) and an intensified, gated photodiode array (Spectroscopy Instruments). Maximum resolution at 300 and 1200 lines/mm was measured to be 0.9 and 0.2 nm, respectively. High resolution fluorescence measurements were recorded by an Andor spectrometer consisting of a polychrometer with 2400 lines/mm holographic grating (Shamrock) and intensified, gated CCD camera (I-Star). The measurements on this system had a maximum resolution of 0.013 nm. Both detection systems were calibrated with a neon lamp (Pen Ray 6032). The samples were cooled to 4 K by a helium refrigerated cryostat (CTI-cryogenics) to improve resolution. For the discrimination of Rayleigh and Raman scattering the minimum gate delay between laser pulse and camera gating was set to 1.0 μs. The gate width of the camera was fixed at 10 ms to ensure the collection of the entire fluorescence signal. Fluorescence lifetime measurements were made with a delay time step between 15 and 200 μs and a total of 60 steps were taken for each lifetime measurement.

3. Results and discussion

3.1 Europium doped $LaPO_4$

Eu doped $LaPO_4$ synthesized by the hydrothermal synthesis described above was analyzed by direct excitation time resolved laser fluorescence spectroscopy. The excitation wavelength was varied in order to probe the ${}^7F_0 \rightarrow {}^5D_0$ energy gap (575–582 nm) directly. This transition is non-degenerate and therefore results in a single peak for each Eu environment. Fig. 1 shows the integrated fluorescence intensity plotted by excitation wavelength. The major species is excited at 578.4 nm and at least one minor species is apparent at 577.5 nm (Fig. 1). After sintering the sample at 1000 °C for 48 h the peak at 578.4 nm remains, but the minor peak shifts from 577.5 to 578.9 nm (not shown). By exciting each species at this unique transition it is possible to obtain emission spectra without interference from multiple species. This is in contrast to the normal UV excitation (394.0 nm) of ${}^7F_0 \rightarrow {}^5L_6$ which excites all Eu species simultaneously.

The emission spectra of the major Eu species (excitation wavelength of 578.4 nm) before and after sintering are shown in Fig. 2. The emission spectrum of the as prepared sample matches well with previously published data [22]. The emission spectra in Fig. 2 show the maximum 3-fold degenerate splitting of the ${}^5D_0 \rightarrow {}^7F_1$ transmission from 585 to 605 nm as expected of a Eu occupying the La site in $LaPO_4$, which has C_1 symmetry. The splitting due to C_1 symmetry of the next transition (${}^5D_0 \rightarrow {}^7F_2$) is expected to be a fully degenerate 5-fold splitting. This was previously unresolved, but calculated to match an emission spectrum similar to that of the as prepared sample (Fig. 2). By increasing the delay time and using a 1200 lines/mm grating it was possible to resolve the 5-fold splitting in the sintered sample between 605 and 635 nm, as was previously calculated [22].

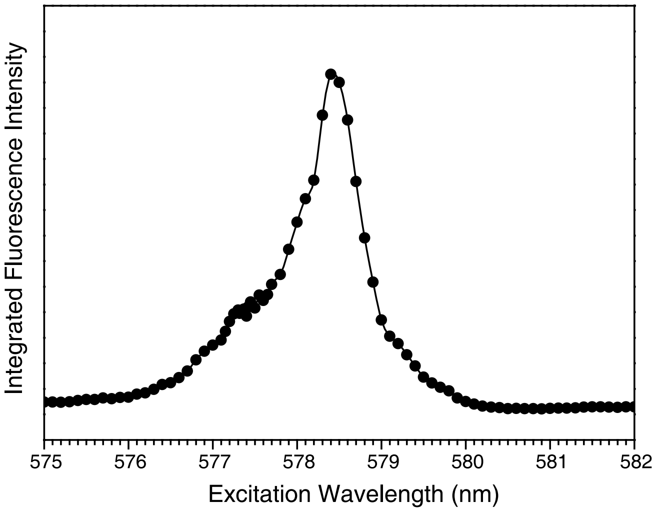

Fig. 1. Excitation spectrum of Eu doped LaPO$_4$ after hydrothermal synthesis indicating $^5D_0 \rightarrow {}^7F_0$ transition for the major species at 578.4 nm and at least one minor species identified at 577.5 nm.

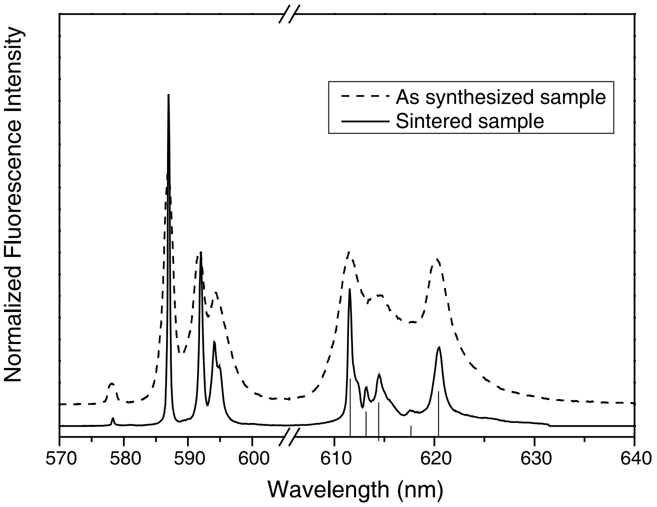

Fig. 2. Emission spectra of the major Eu species from direct excitation at 578.4 nm before and after sintering LaPO$_4$. The sintered sample confirms previously calculated peak positions (indicated with lines) between 605 and 625 nm [22].

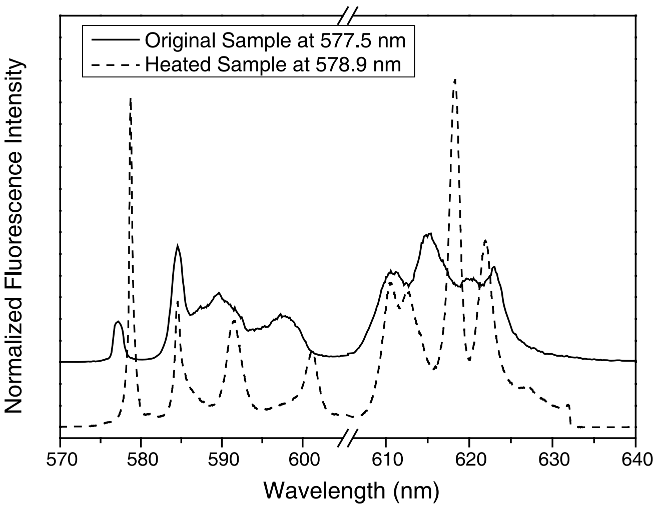

Fig. 3. Emission spectra of the minor Eu species in LaPO$_4$ from direct excitation before (577.5 nm excitation) and after (578.9 nm excitation) sintering illustrating a change in the minor Eu environment due to heating.

The sintered sample can be compared to that of the as prepared sample in Fig. 2. There is no significant change in the spectra due to sintering indicating that Eu occupies the La site in the as prepared sample despite the low temperature synthesis.

A minor species was also identified before and after sintering. The excitation wavelength for this species changed from 577.5 nm before sintering to 578.9 nm after sintering indicating a change in the local environment of the Eu. The species at 577.5 nm was no longer evident after heating the sample. This change is also evident by the difference in the emission spectra of these two Eu species (Fig. 3). Both emission spectra in Fig. 3 indicate low symmetry Eu species with a fully degenerate 3-fold splitting of the $^5D_0 \rightarrow {}^7F_1$ transition from 585–605 nm. The $^5D_0 \rightarrow {}^7F_2$ transition is likely fully degenerate 5-fold split in both species although this is only clearly resolved in the heat treated sample from 605–635 nm (Fig. 3). The heat treated sample also shows a relative increase in the transitions to $^7F_0$ (578–580 nm) and $^7F_2$ (605–635 nm) as compared to the $^7F_1$ (585–605 nm) indicating an increase in the asymmetrical ligand field strength upon sintering (Fig. 3). Because there is only one cation site in LaPO$_4$ the minor species is believed to be due to hydroxide interstitials in the LaPO$_4$ phase that can not be removed by acid treatment. This would explain the observed increase in ligand strength and change in Eu environment upon heating due to the conversion of hydroxide to oxide in the material. It is important to note that while the major and minor species can be probed individually they are both present before and after sintering.

Fluorescence lifetimes for Eu were measured by exciting to the $^5L_6$ level and fitting the decay of the fluorescence to Eq. (1) for bi-exponential decay.

$$I_t = A_1 \exp(-k_1 t) + A_2 \exp(-k_2 t) \quad (1)$$

In Eq. (1), I_t is the integrated fluorescence intensity at time t. By exciting all Eu species it was possible to get a relative abundance for each species by the ratio of quantities A_1 and A_2 assuming equal fluorescence intensity from both species. The reciprocal observed lifetime (k) in ms^{-1} is used in the linear relationship developed by Horrocks and Sudnick [26] to relate the fluorescence lifetime of Eu to the number of waters, $n(H_2O)$, in the immediate coordination sphere according to Eq. (2). The typical error associated with this measurement is ± 0.5 waters.

$$n(H_2O) = 1.07k_{obs} - 0.62 \quad (2)$$

The observed lifetime can then be assigned to a species through lifetime measurements done by direct excitation, thereby isolating one species from the other. The fluorescence lifetimes, relative abundance, and corresponding number of waters for each Eu species before and after heating are summarized in Table 1. The major species found at an excitation wavelength of 578.4 nm has a long fluorescence lifetime before (5.2 ms) and after (3.6 ms) heat treatment indicating that there are no waters in the immediate coordination sphere, as was expected for Eu substituted on a La

Table 1. Sumary of data obtained from fluorescence decay measurements on Eu doped $LaPO_4$ and corresponding number of waters in the first coordination sphere as calculated by Eq. (2).

	Relative abundance (%)	Lifetime (ms)	# H_2O
Major Eu site (578.4 nm) in as prepared sample	70	5.2	0.0
Major Eu site (578.4 nm) in sintered sample	70	3.6	0.0
Minor Eu site (577.5 nm) in as prepared sample	30	0.95	0.5
Minor Eu site (578.9 nm) in sintered sample	30	1.4	0.1

site in the $LaPO_4$ structure. These fluorescence lifetimes correspond to −0.41 and −0.32 waters by Horrocks equation. While negative waters have no physical meaning, it illustrates the difference in these lifetimes is trivial. The minor Eu site before heat treatment has a lifetime of 0.95 ms, which correlates to 0.5 waters supporting the hypothesis of Eu species coordinated to a hydroxide interstitial. Further evidence of this is found as the lifetime is longer after heat treatment. The lifetime after heat treatment is 1.4 ms corresponding to 0.1 waters, which is an indication that the hydroxide is being converted to oxygen by heating the sample.

3.2 Curium doped $LaPO_4$

Cm doped $LaPO_4$ was analyzed in a similar way to that of the Eu doped sample by direct excitation time resolved laser spectroscopy. The transition used to probe Cm in this study is the $^8S_{7/2} \rightarrow {}^6D_{7/2}$ excitation and emission ($^6D_{7/2} \rightarrow {}^8S_{7/2}$). This is complicated by splitting of both the $^8S_{7/2}$ ground state and the $^6D_{7/2}$ excited state. The splitting of the $^6D_{7/2}$ excited state is on the order of hundreds of cm^{-1} and is therefore easy to distinguish [27]. For the current study only the so-called A_1 transition to and from the lowest $^6D_{7/2}$ excited state will be discussed. The ground state $^8S_{7/2}$ multiplet has a maximum of four components in the absence of a magnetic field and has been found to have an energy splitting of up to 66 cm^{-1} [28].

In the case of the as synthesized sample this ground state splitting was not resolved. The main excitation peak was found at 602.5 nm while a shoulder was evident around 601.7 nm indicating a minor species (Fig. 4). Emission spectra from UV excitation (396.6 nm) and direct excitation (600–604 nm) were measured for the as prepared $LaPO_4$ doped with Cm (not shown) and were found to correspond with the excitation spectrum taken before heating (Fig. 4). These results compare well with the sample doped with Eu (Fig. 1). In both Eu and Cm doped $LaPO_4$ there is a minor species at slightly higher energy as compared to that of the major species in the as prepared sample. There is a relatively large bathochromic shift for the major Cm site due to the strong complexation of the PO_4^{3-} group as compared to the 9-fold coordinated Cm^{3+} aquo ion found at 593.8 nm [29]. It is not, however, red shifted to the extent of the Cm doped 8-fold coordinated $LuPO_4$, found at 605 nm [24]. This is further evidence that the major Cm site is 9-fold coordinated in the La site of the $LaPO_4$ crystal structure.

Lifetimes were measured from UV excitation (396.6 nm) to obtain relative abundance from the fit to Eq. (1) and then assigned to each peak by measurements with direct excitation as previously described for Eu:$LaPO_4$. The reciprocal fluorescence decay lifetime (k) in ms^{-1} of Cm can be linearly related to the number of waters in the first coordination sphere, $n(H_2O)$, by the equation developed by Kimura and Choppin [30] (Eq. 3). The typical error associated with this measurement is ± 0.5 waters.

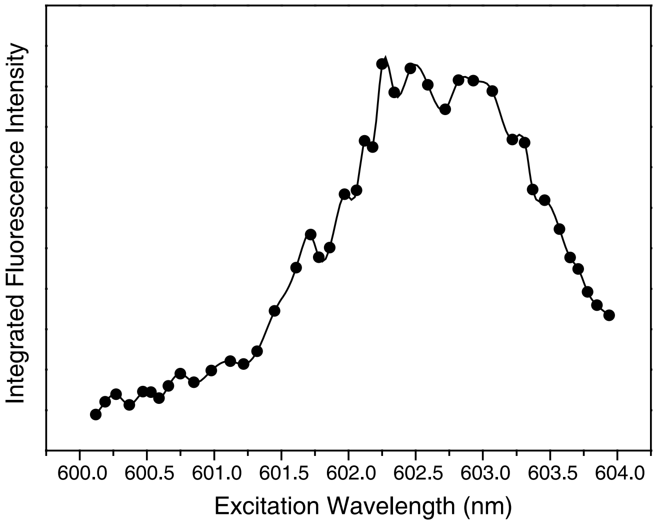

Fig. 4. Excitation spectrum of Cm doped $LaPO_4$ after hydrothermal-synthesis indicating the $^8S_{7/2} \rightarrow {}^5D_{7/2}$ transition for the major species at 602.5 nm and a minor species at 601.7 nm.

$$n(H_2O) = 0.65k_{obs} - 0.88 \tag{3}$$

The information obtained from fluorescence lifetime measurements on Cm doped $LaPO_4$ is summarized in Table 2. The major species has a long fluorescence lifetime of 1.7 ms corresponding to an absence of water in the immediate coordination sphere. This is consistent with Eu studies which identified the site as the La site of $LaPO_4$. Therefore, the major Cm species at 602.5 nm is concluded to be the La site of $LaPO_4$ as previously supposed from the peak position of the emission spectrum. The minor species has a faster lifetime of 0.52 ms indicating 0.5 waters, or a hydroxide, similar to the minor species in the Eu:$LaPO_4$. This is suspected of being an incorporated Cm that is complexed to a hydroxide interstitial that could not be removed by acid treatment.

After heating the sample to 1000 °C for 48 h there was no evidence of a minor species. The main peak remains centered at 602.5 nm and some structure is evident in the peak due to ground state splitting of the $^8S_{7/2}$ state after sintering (Fig. 5). In this excitation spectrum four peaks can be observed, but there is also clear shoulders present on several peaks indicating more than the maximum four components of the $^8S_{7/2}$ ground state. This is further discussed in high resolution measurements below. The absence of a minor species after heating the Cm:$LaPO_4$ sample as compared to

Table 2. Sumary of data obtained from fluorescence decay measurements on Cm doped $LaPO_4$ and corresponding number of waters in the first coordination sphere as calculated by Eq. (3).

	Relative abundance (%)	Lifetime (ms)	# H_2O
Major Cm site (602.5 nm) in as prepared sample	70	1.7	0.0
Minor Cm site (601.7 nm) in as prepared sample	30	0.52	0.4
Major Cm site (602.5 nm) in sintered sample	100	1.2	0.0

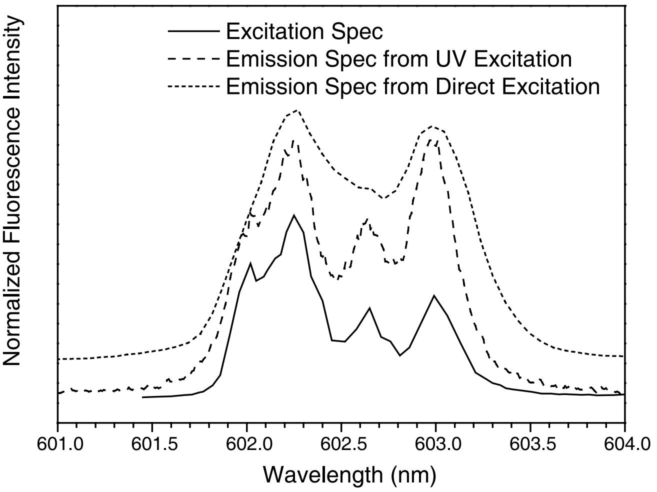

Fig. 5. A comparison of the excitation spectrum (solid line), emission spectrum from UV excitation at 396.6 nm (dashed line), and low resolution emission spectrum from direct excitation at 602.5 nm (dotted line) of Cm doped $LaPO_4$ after sintering, which shows unresolved but consistent energy splitting of the ground state.

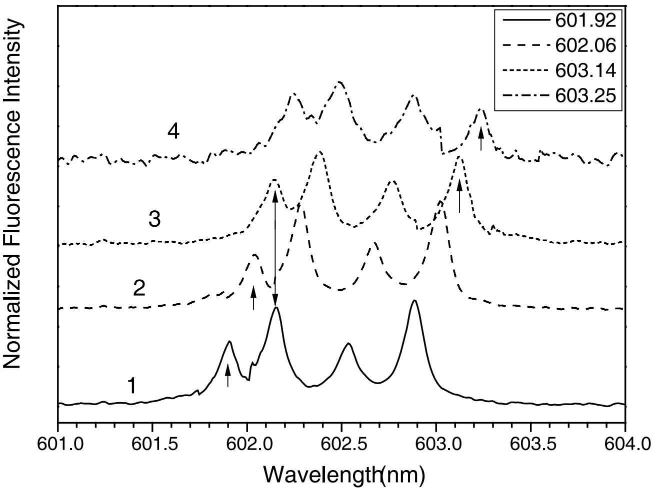

Fig. 6. High resolution emission spectra from direct excitation of Cm in sintered $LaPO_4$. Single arrows indicate wavelength of direct excitation used to obtain that emission spectrum as listed in the legend. Double arrow indicates position of direct excitation that would excite multiple Cm species yielding more than the maximum four peaks allowed by the ground state splitting of a single species.

the Eu:$LaPO_4$ sample is most likely due to the difference in concentrations (5% Eu as compared to 7 ppm Cm). The emission spectra from UV and direct excitation are compared to the excitation spectra in Fig. 5. The emission spectrum from direct excitation produces the shape of both the excitation spectrum and the emission spectrum from UV excitation indicating that all peaks are from a single Cm site within the $LaPO_4$.

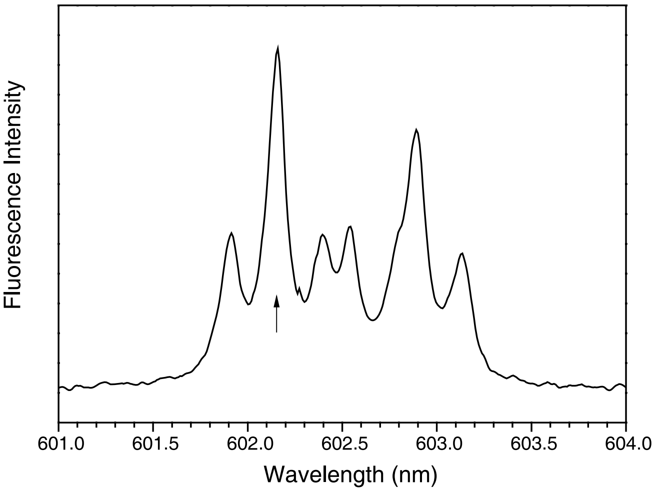

Fig. 7. High resolution emission spectra from direct excitation at 602.18 nm (as was indicated by double arrow in Fig. 6) in sintered Cm:$LaPO_4$ showing more emission peaks than can be explained by the ground state splitting of single Cm species. Single arrow indicates the wavelength of direct excitation used to obtain that emission spectrum.

Definitive proof of a single Cm site after heating was obtained by measuring the fluorescence decay lifetimes. Both UV excitation (396.6 nm) and direct excitation at four different wavelengths (602.0–603.0 nm) was used in lifetime measurements. All fluorescence decays were monoexponential indicating a single Cm site. The fluorescence lifetime measured at each wavelength was 1.2 ms corresponding to a complete loss of the hydration sphere (Eq. 3), consistent with substitution on a La site as was previously shown for Eu.

In order to resolve the ground state splitting high resolution emission spectra were taken under direct excitation (wavelength monitored to within 0.001 nm) with an Andor camera system capable of 0.013 nm resolution (2400 lines/mm grating). By systematically stepping through excitation wavelengths (601.5–603.5 nm), it was possible to excite four different species, each with four-fold splitting (Fig. 6). It should be noted that the difference between these four species is extremely small and can only be seen by such a precise measurement. This has previously been observed in Cm doped xenotime structure and was labeled as “satellites” [24, 25]. Four satellites were also observed in the xenotime structure although individual spectra from each were not resolved due to overlapping excitation energies. The current study was successful in isolating each satellite through direct excitation (Fig. 6). Arrows in Fig. 6 indicate positions where it is possible to excite a single Cm species and obtain the subsequent 4-fold split emission spectra. Other excitation wavelengths yield a combination of species that can be predicted from the individual spectra.

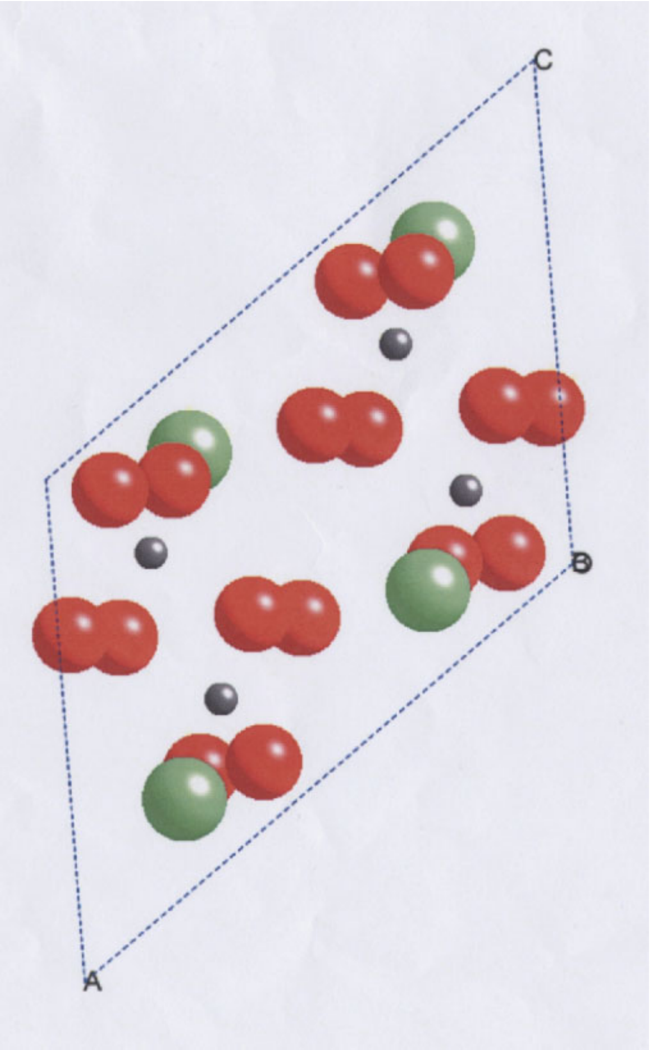

Fig. 8. Crystal structure of natural monazite illustrating the four La atoms (shown as green spheres). Oxygens are shown as red spheres and phosphorous as small grey spheres.

For instance the double arrow on Fig. 6 would be a direct excitation of 602.18 nm. This excitation energy would excite the second peak of species 1 and the first peak of species 3 (Fig. 6). By exciting an overlapping peak of these two species a total of six peaks can be observed in the emission spectrum as seen in Fig. 7.

There are two explanations for this phenomenon found in literature for the Cm:$LuPO_4$ system. One is that self heating due to the decay of Cm-244 and local heating by the laser result in electron population in all ${}^8S_{7/2}$ levels [25]. This is unlikely in the current study due to the use of Cm-248, which has a very low specific activity. There is also evidence in the current study, although not resolved, of satellite peaks in the emission spectra from UV excitation (Fig. 5), which cannot be explained by this effect. The second explanation presented in literature for satellite peaks found in Cm:$LuPO_4$ is attributed to impurities or defects within the crystal structure [24]. This is the more likely cause of slightly different environments of Cm, however, the occurrence of four environments in both systems suggests more than random effects of a deviation from the ideal crystal structure. The similar degree of splitting, ratio of peak heights in the emission spectra of each satellite, and their proximity to each other suggest that the Cm environment is almost identical in all four satellites (Fig. 6). All four satellite sites show the same lifetime of 1.2 ms. Therefore, the hypothesis suggested in the present work is that this is a difference in the four La sites within a unit cell of the $LaPO_4$ structure due to a digression from the ideal crystal structure. This would also explain the observations in literature for the $LuPO_4$ system, which also has four symmetry equivalent cation sites [24, 25]. The crystal structure of $LaPO_4$ can be seen in Fig. 8. Using this explanation, the present manuscript refers to the sintered Cm:$LaPO_4$ as having a single Cm site as would be defined in the classical crystal chemistry description as the La site with four Cm environments or satellites as discovered by high precision spectroscopy measurements presented here. The difference in these four environments is mostly likely due to impurities or defects within the crystal structure resulting in a difference in the four cation sites within a unit cell.

4. Conclusions

This manuscript presents the results of site-selective time resolved laser fluorescence measurements of Eu and Cm doped $LaPO_4$ as prepared by hydrothermal synthesis and subsequent sintering. The major site before and after sintering was found to be the same despite the lower temperature synthesis method. The emission spectra from the major Eu site shows a resolved and fully degenerate 5-fold splitting of the F_2 transition, confirming previously calculated data [22] and proving that Eu was incorporated in the La site through isomorphic substitution. This was compared to Cm spectroscopic data to conclude that the major site in Cm:$LaPO_4$ is also Cm substituted on the La site of $LaPO_4$. High resolution direct excitation time resolved laser fluorescence spectroscopy was used to show that this single site of Cm was actually four slightly different environments or satellites. This is hypothesized to be a difference in the four La sites within a $LaPO_4$ unit cell due to a deviation from the ideal structure, which would break the equivalence of the La atom sites. A minor site was identified in both Eu and Cm samples. The fluorescence lifetime and emission data suggests that the minor site is coordinated to a single hydroxide interstitial. This minor site persisted in the Eu doped sample after sintering, however, the fluorescence lifetime and emission spectra changed. This change in spectra was attributed to a change in the hydroxide interstitial due to heat treatment. While spectroscopic measurements were performed at cryogenic temperatures (4 K) there is no evidence of a phase change. Therefore, these conclusions can be expanded to ambient and the slightly elevated temperature of a nuclear waste form. It is evident from this study that minor species due to hydroxide impurities must be taken into consideration given the proposed synthesis route. The appearance of satellite species also challenges the simple notion of isomorphic substitution of an ideal structure.

Acknowledgment. The authors thank Sebastian Büchner for technical assistance with TRLFS measurements. This work was co-financed by the Helmholtz Gemeinschaft Deutscher Forschungszentren (HGF) by supporting the Helmholtz-Hochschul-Nachwuchsgruppe “Aufklärung geochemischer Reaktionsmechanismen an der Wasser/Mineralphasen

Grenzfläche”. This work also was supported by the Ministerium für Innovation, Wissenschaft, Forschung und Technologie (MIWFT) des Landes Nordrhein-Westfalen; AZ: 323-005-0911-0129.

References

1. Trocellier, P.: Chemical durability of high level nuclear waste forms. Ann. Chim. Sci. Mat. **26**, 113 (2001).
2. Lumpkin, G. R.: Ceramic waste forms for actinides. Elements **2**, 365 (2006).
3. Weber, W. J., Navrotsky, A., Stefanovsky, S., Vance, E. R., Vernaz, E.: Materials science of high-level nuclear waste immobilization. MRS Bull. **34**, 46 (2009).
4. Donald, I. W., Metcalfe, B. L., Taylor, R. N. J.: The immobilization of high level radioactive wastes using ceramics and glasses. J. Mater. Sci. **32**, 5851 (1997).
5. Cohen, B. L.: High-level radioactive waste from light-water reactors. Rev. Mod. Phys. **49**, 1 (1977).
6. Deschanels, X., Picot, V., Glorieux, B., Jorion, F., Peuget, S., Roudil, D., Jégou, C., Broudic, V., Cachia, J. N., Advocat, T., Den Auwer, C., Fillet, C., Coutures, J. P., Hennig, C., Scheinost, A.: Plutonium incorporation in phosphate and titanate ceramics for minor actinide containment. J. Nucl. Mater. **352**, 233 (2006).
7. Bregiroux, D., Belin, R., Valenza, P., Audubert, F., Bernache-Assolant, D.: Plutonium and amercium monazite materials: solid state synthesis and X-ray diffraction study. J. Nucl. Mater. **366**, 52 (2007).
8. Glorieux, B., Montel, J. M., Matecki, M.: Synthesis and sintering of a monazite-brabantite solid solution ceramics using metaphosphate. J. Eur. Ceram. Soc. **29**, 1679 (2009).
9. Montel, J.-M., Glorieux, B., Seydoux-Guillaume, A.-M., Wirth, R.: Synthesis and sintering of a monazite-brabantite solid solution ceramic for nuclear waste storage. J. Phys. Chem. Solids **67**, 2489 (2006).
10. Seydoux-Guillaume, A.-M., Paquette, J. L., Wiedenbeck, M., Montel, J. M., Heinrich, W.: Experimental resetting of the U-Th-Pb system in monazite. Chem. Geol. **191**, 165 (2002).
11. Seydoux-Guillaume, A.-M., Wirth, R., Ingrin, J.: Contrasting response of $ThSiO_4$ and monazite to natural irradiation. Eur. J. Mineral. **19**, 7 (2007).
12. Burakov, B. E., Yagovkina, M. A., Garbuzov, V. M., Kitsay, A. A., Zirlin, V. A.: Self-irradiating of monazite ceramics: contrasting behavior of $PuPO_4$ and $(La, Pu)PO_4$ doped with Pu-238. (Hanchar, J. M., ed.) Scientific Basis for Nuclear Waste Management XXVIII, Springer, Berlin (2004), Vol. 824, p. 219.
13. Meldrum, A., Boatner, L. A., Ewing, R. C.: Displacive radiation effects in the monazite- and zircon-structure orthophosphates. Phys. Rev. B **56**, 13805 (1997).
14. Karioris, F. G., Gowda, K. A., Cartz, L.: Heavy ion bombardment of monoclinic $ThSiO_4$, ThO_2 and monazite. Radiat. Eff. Lett. **58**, 1 (1981).
15. Meldrum, A., Boatner, L. A., Ewing, R. C.: Electron irradiation-induced nucleation and growth in amorphous $LaPO_4$, $ScPO_4$, and zircon. J. Mater. Res. **12**, 1816 (1997).
16. Picot, V., Deschanels, X., Peuget, S., Glorieux, B., Seydoux-Guillaume, A. M., Wirth, R.: Ion beam radiation effects in monazite. J. Nucl. Mater. **381**, 290 (2008).
17. Lisiecki, R., Solarz, P., Dominiak-Dzik, G., Ryba-Romanowski, W., Sobczyk, M., Černý, P., Šulc, J., Jelínková, H., Urata, Y., Higuchi, M.: Comparative optical study of thulium-doped YVO_4, $GdVO_4$, and $LuVO_4$ single crystals. Phys. Rev. B. **74**, 035103 (2006).
18. Fan, W., Bu, Y., Song, X., Sun, S., Zhao, X.: Selective synthesis and luminescent properties of monazite- and zircon-type $LaVO_4 : Ln$ ($Ln = Eu$, Sm, and Dy) nanocrystals. Cryst. Growth Des. **7**, 2361 (2007).
19. Niu, N., Piaoping, Y., Wang, Y., Wang, W., He, F., Gai, S., Wang, D.: $LaPO_4 : Eu^{3+}$, $LaPO_4 : Ce^{3+}$, and $LaPO_4 : Ce^{3+}$, Tb^{3+} nanocrystals: Oleic acid assisted solvothermal synthesis, characterization, and luminescent properties. J. Alloys Compd. **509**, 3096 (2011).
20. Byrappa, K., Devaraju, M. K., Paramesh, J. R., Basavalingu, B., Soga, K.: Hydrothermal synthesis and characterization of $LaPO_4$ for bio-imaging phosphors. J. Mater. Sci. **43**, 2229 (2008).
21. Ternane, R., Ferid, M., Panczer, G., Trabelsi-Ayadi, M., Boulon, G.: Site-selective spectroscopy of Eu^{3+}-doped orthorhombic lanthanum and monoclinic yttrium polyphosphates. Opt. Mater. **27**, 1832 (2005).
22. Meyssamy, H., Riwotzki, K., Kornowski, A., Naused, S., Haase, M.: Wet-chemical synthesis of doped colloidal nanomaterials: particles and fibers of $LaPO_4$:Eu, $LaPO_4$:Ce, and $LaPO_4$:Ce,Tb. Adv. Mater. **11**, 840 (1999).
23. Cavellec, R., Lucas, C., Simoni, E., Hubert, S., Edelstein, N.: Structural characterization of sorption complexes of Cm(III) at the phosphate minerals-solution interface using laser spectrofluorimetry. Radiochim. Acta **82**, 221 (1998).
24. Murdoch, K. M., Edelstein, N. M., Boatner, L. A., Abraham, M. M.: Excited state absorption and fluorescence line narrowing studies of Cm^{3+} in $LuPO_4$. J. Chem. Phys. **105**, 2539 (1996).
25. Liu, G. K., Li, S. T., Zhorin, V. V., Loong, C.-K., Abraham, M. M., Boatner, L. A.: Crystal-field splitting, magnetic interaction, and vibronic excitations of $^{244}Cm^{3+}$ in YPO_4 and $LuPO_4$. J. Chem. Phys. **109**, 6800 (1998).
26. Horrocks Jr., W. D., Sudnick, D. R.: Lanthanide ion probes of structure in biology. Laser induced luminescence decay constants provide a direct measure of the number of metal-coordinated water molecules. J. Am. Chem. Soc. **101**, 334 (1979).
27. Edelstein, N. M.: Comparison of the electronic structure of lanthanides and actinides. J. Alloys Compd. **223**, 197 (1995).
28. Edelstein, N. M., Klenze, R., Fanghänel, T., Hubert, S.: Optical properties of Cm(III) in crystals and solutions and their application to Cm(III) speciation. Coord. Chem. Rev. **250**, 948 (2006).
29. Lindqvist-Reis, P., Klenze, R., Schubert, G., Fanghänel, T.: Hydration of Cm^{3+} in aqueous solution from 20 to 200 °C. A time-resolved laser fluorescence spectroscopy study. J. Phys. Chem. B **109**, 3077 (2005).
30. Kimura, T., Choppin, G. R.: Luminescence study on determination of the hydration number of Cm(III). J. Alloys Compd. **213/214**, 313 (1994).